Fluorescence Quenching | Hot Paper

How to cite:
International Edition: doi.org/10.1002/anie.202101730
German Edition: doi.org/10.1002/ange.202101730

Implications of Quenching-to-Dequenching Switch in Quantitative Cell Uptake and Biodistribution of Dye-Labeled Nanoparticles

*Guangze Yang[+], Yun Liu[+], Yue Hui, Tengjisi, Dong Chen, David A. Weitz, and Chun-Xia Zhao**

Abstract: *A general strategy to carry out cell uptake and biodistribution studies is to label nanoparticles (NPs) with a fluorescent dye. However, the comparative study of different dye-loaded NPs remains difficult owing to uncontrolled dye quenching and de-quenching. Here we compared two types of dye-labeled NPs and demonstrated their distinct properties. NPs with dye molecules at a solid state suffer from dye quenching, so the dye release and/or NP degradation in biological environments leads to a several-fold increase of fluorescence intensity despite the same amount of NPs, owing to the state switch from quenching to de-quenching. In contrast, NPs with dye molecules at a soluble state exhibit no quenching effect. To standardize the comparative study, we propose two possible solutions: using lower dye loading or using medium analysis for quantifying cell uptake of NPs. This work provides valuable insights into selecting valid quantification methods for bio-nano studies.*

Introduction

Numerous studies have reported the development of a wide variety of nanoparticles (NPs) for drug delivery,[1] but standardization is lacking in the field which makes it difficult to compare different nanoparticle systems. Therefore, the establishment of protocols for quantitative comparison of different nanoparticle systems becomes urgent and imperative. For preclinical evaluation, cell uptake and biodistribution studies have become a routine for studying nanoparticle drug delivery.

Fluorescent labeling has been widely used in evaluating cell uptake and biodistribution of various NPs.[2] Fluorescence imaging serves as a powerful tool for monitoring NPs in vitro and in vivo.[3] More importantly, the visualization of NPs offers more sensible and direct evidence.[4] NPs are normally labeled with fluorescent dyes either through encapsulation inside the particles or conjugation on the particle surface.[5] For example, fluorescent dyes can be encapsulated in polymeric NPs and liposomes through hydrophobic interactions.[6] They can also be dissolved in a hydrophobic phase such as oil to make emulsion-based NPs.[7]

An underlying assumption is that the fluorescence intensity correlates positively with the amounts of NPs accumulated in cells or tissues and organs in mice. However, this is not necessarily true for some NP systems, let alone the comparison of different nano-systems, as many factors could affect the fluorescence intensity in vitro and in vivo. For example, the dispersion state of dye molecules in NPs gives a very different readout. When most dyes present in the NPs at a solid or an aggregate state, the aggregation-caused-quenching (ACQ) effect comes into play.[8] It has been reported that cells incubated with the same polymer NPs having low (1 wt %) and high (3.6 wt %) dye loading yielded opposite results in biodistribution study,[9] due to fluorescence quenching, dequenching, and signal saturation.[10] Some studies have utilized these quenching and de-quenching effects at high dye loading for stimuli-responsive sensing applications[11] as well as monitoring dye release from polymer NPs.[12] However, the quenching effect at low dye loadings has rarely been taken into consideration during experimental design. More surprisingly many studies did not even mention the dye loading of NPs,[13] which could lead to wrong interpretation of data thus misleading conclusions.[9] Actually, many dyes suffer from the ACQ effect,[14] and dyes confined in solid NPs are often quenched to some extent even at a commonly used loading dosage of 0.1–1 % mainly because of dye aggregation.[15]

In this study, we compared two different kinds of dye-labeled nanoparticles using one widely used dye 1,1′-dioctadecyl-3,3,3′3′-tetramethylindocarbocyanine perchlorate (DiI), that is, DiI-loaded polymer NPs (DiI@Polymer) and DiI loaded oil-core silica-shell NPs (DiI@Oil). For the DiI@Polymer NPs, DiI molecules are trapped inside the solid polymer NPs at a solid state, while for the DiI@Oil NPs, DiI molecules are dissolved in the oil phase at a soluble state. To our great surprise, we observed distinct cell uptake and biodistribution results for the DiI@Polymer and DiI@Oil NPs. To avoid the interference from continuing NP cell

[*] Dr. G. Yang,[+] Dr. Y. Liu,[+] Dr. Y. Hui, Tengjisi, Prof. Dr. C.-X. Zhao
Australian Institute for Bioengineering and Nanotechnology, University of Queensland
St. Lucia, Queensland (Australia)
E-mail: z.chunxia@uq.edu.au
Prof. Dr. D. Chen
Institute of Process Equipment, College of Energy Engineering, Zhejiang University
Hangzhou (China),
and
State Key Laboratory of Fluid Power and Mechatronic Systems, Zhejiang University
Hangzhou (China)
Prof. Dr. D. A. Weitz
John A. Paulson School of Engineering and Applied Sciences, Harvard University
Cambridge, MA (USA),
and
Department of Physics, Harvard University
Cambridge, MA (USA)
[+] These authors contributed equally to this work.
Supporting information and the ORCID identification number(s) for the author(s) of this article can be found under: https://doi.org/10.1002/anie.202101730.

uptake thus increasing fluorescence intensity, we designed a one-off experiment. Basically, NPs are incubated with cells for 15 min, followed by washing to remove free NPs. Then cells containing the internalized NPs are collected and incubated further, and the fluorescence intensity is monitored over time. As the NP number does not change, it is expected that the fluorescence intensity does not change at the beginning followed by a gradual decrease due to dye degradation. The DiI@Oil NPs behaved as we expected. However, the DiI@Polymer NPs exhibited a completely opposite phenomenon showing a several-fold increase of the fluorescence intensity.

The striking fluorescence intensity increase of the DiI@-Polymer NPs was carefully investigated using the Förster resonance energy transfer (FRET) method. We found that the dye release and/or NP degradation in biological environments resulted in a quenching-to-dequenching switch of the DiI loaded in the NPs. In contrast, the DiI@Oil NPs have no quenching effect because the DiI was dissolved in the oil core as a non-quenched-soluble state, therefore their fluorescence intensity remained stable during incubation. Similar phenomena were also observed in in vivo study. These findings have critical implications in using fluorescent labeling in cell and animal studies of NPs. To address this challenge, we propose two different approaches for future cell and animal comparative studies.

Results and Discussion

We fabricated DiI@Polymer NPs using the most commonly used di-block copolymer poly(lactic-co-glycolic acid)-poly(ethylene glycol) (PLGA-PEG; Supporting Information, Figure S1 and Table S1). A model hydrophobic dye DiI was co-precipitated with the polymer $PLGA_{55k}$-PEG_{5k} at a common dye loading of 1 wt%. We synthesized DiI@Oil NPs using a nano-emulsion templating method (Supporting Information, Figure S1 and Table S1).[7b,16] DiI was dissolved in the oil phase followed by emulsification and biosilicification thus forming DiI-loaded oil-core silica-shell nano-capsules. The DiI molecules in the DiI@Polymer NPs and DiI@Oil NPs are in different states, with the former in a solid state and the latter in a soluble state. Their different states in NPs have profound implications in fluorescent quantification of cell uptake and biodistribution studies of NPs.

The DiI@Polymer ($PLGA_{55k}$-PEG_{5k}) and DiI@Oil NPs were incubated with an ovarian cancer cell line SKOV3 for 15 min, followed by washing with phosphate-buffered saline (PBS) three times to remove free NPs (Figure 1 a,b). Then cells containing the internalized NPs were collected (regarded as 0 h) and incubated in medium solutions for 8 h (denoted as one-off cell uptake method). The fluorescence intensity was monitored (Figure 1 c,d; Supporting Information, Figures S2 and S3). At the beginning (0 h), the DiI@Polymer NPs were observed mainly around the cell membrane with weak fluorescence. Then at 2 h, the cytoplasm of cells was illuminated with brighter fluorescence (shown as green color). More interestingly, the fluorescence intensity increased significantly over time from 2 h to 8 h. After 8 h, the fluorescence intensity started to decrease probably due to dye degradation (Supporting Information, Figure S4). This is counterintuitive as the numbers of DiI@Polymer NPs in the cells remained near constant. The significant increase in fluorescence intensity was not due to the increased NP uptake. This significant increase of the fluorescence intensity during incubation occurred for other dyes as well, for example, the green fluorescent, lipophilic carbocyanine dye 3,3′-dioctadecyloxacarbocyanine perchlorate (DiO; Supporting Information, Figure S5). In contrast, the DiI@Oil NPs demonstrated a bright fluorescence around the cell membrane at 0 h. Over time, the fluorescent signal moved from the cell membrane to the cell cytoplasm, and the fluorescence intensity slightly decreased with time. Also, the quantitative flow cytometry results correspond well with the qualitative confocal laser scanning microscopy (CLSM) images (Figure 1 e). The fluorescence intensity of DiI@Polymer NPs incubated with SKOV3 cells increased 2.6 times from 0 to 8 h, while DiI@Oil NPs only exhibited a slight decrease (16%) over time (Figure 1 f).

For both the DiI@Polymer and DiI@Oil NP systems, NP number associated with the SKOV3 cells remained near constant as the free NPs were removed after the initial 15 min incubation. In addition, the efflux of dye was minimal (2% at 2 h incubation; Supporting Information, Figure S6) and the cells were washed each time before the measurement to minimize the effect of efflux. The gradual decrease of the DiI@Oil NP fluorescence suggested the slow degradation of dyes in cells. While the dramatic fluorescence increase of the DiI@Polymer in cells was unexpected as the DiI loading (1 wt%) was low, dye quenching due to ACQ should have been avoided. However, when we compared the quantum yield (Φ) of the DiI@Polymer NPs having different dye loading (Figure 1 g), strikingly, 1 wt% DiI loading in the DiI@Polymer showed a significant ACQ with a quantum yield of 13%. And the ACQ diminished with the decreasing of dye loading until 0.02 wt% which had a similar quantum yield as 0.01 wt% of dye loading ($\Phi = 73\%$). Based on this experiment, it is clear that the DiI@Polymer NPs suffer from considerable ACQ at the DiI loading of 1 wt%. Therefore, the significant fluorescence increase of the DiI@Polymer in cells was probably attributed to the dequenching of the solid state DiI over time. This quenching-to-dequenching switch of the DiI molecules during cell incubation resulted in the increase of the fluorescence intensity despite the constant number of DiI@Polymer NPs in the cells.

To further investigate the in vitro behavior of the DiI@Polymer NPs (1 wt% DiI loading) during the quenching-to-dequenching switch, the fluorescence intensities of three different DiI@Polymer ($PLGA_{10-15k}$, $PLGA_{10k}$-PEG_{5k}, $PLGA_{55k}$-PEG_{5k}) NPs were compared (Figure 2 a; Supporting Information, Figures S1 and S7, Table S1). All the three NPs demonstrated a significant increase of the fluorescence intensity during incubation despite the near constant NP numbers in cells, while the fluorescence intensity of $PLGA_{10-15k}$ NPs increased much faster than those of the $PLGA_{10k}$-PEG_{5k} and $PLGA_{55k}$-PEG_{5k} NPs, showing a 4.7-fold increase at 8 h in contrast to a less than a three-fold increase of the DiI@$PLGA_{55k}$-PEG_{5k} NPs. It may be attributed to the slower

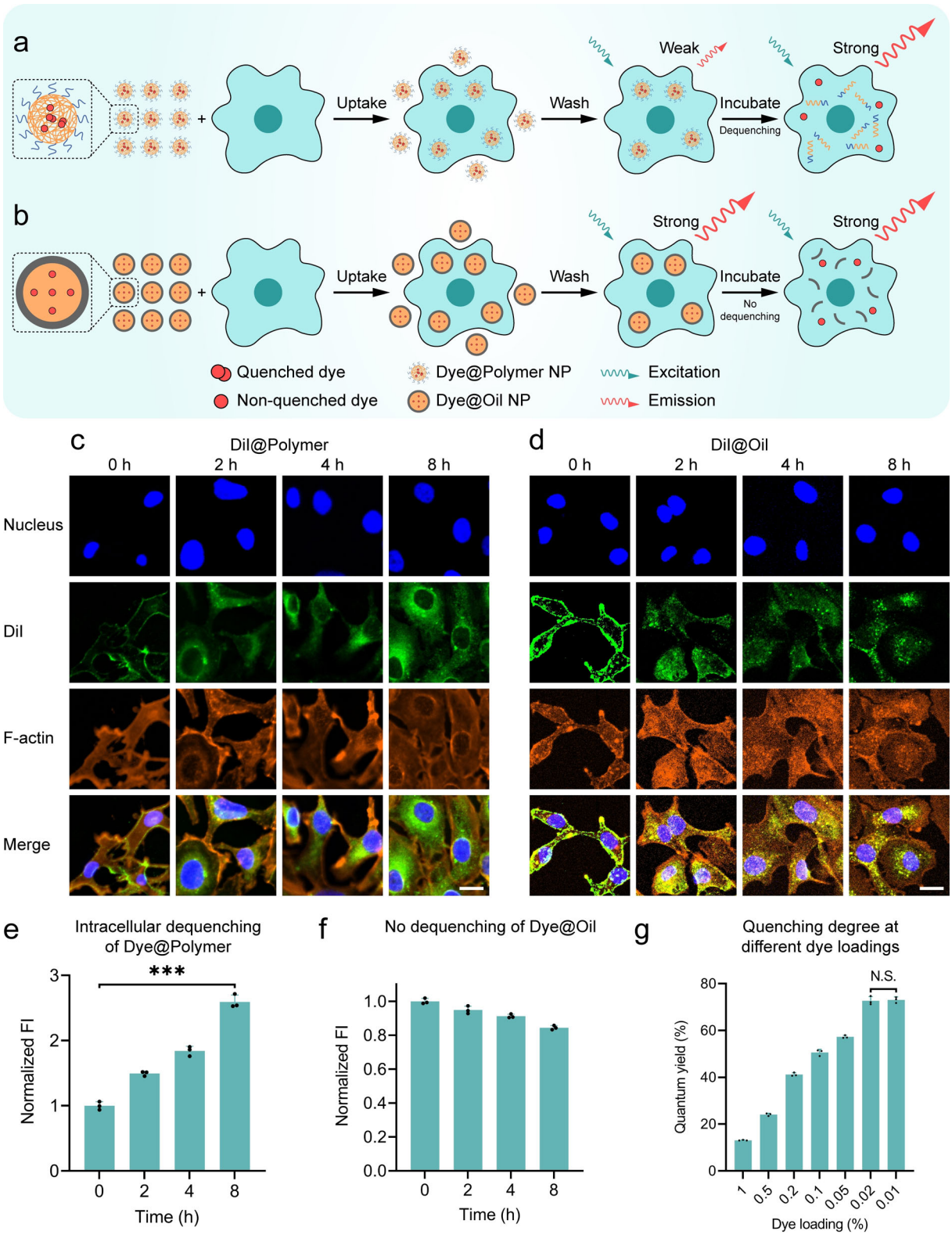

Figure 1. Comparison of two nanoparticle systems: DiI@Polymer NPs and DiI@Oil NPs. a) Schematic illustration of the one-off cell uptake experiment of the DiI@Polymer NPs. NPs are taken up by cells and then free NPs are washed away. The cells show weaker fluorescence at this beginning but stronger fluorescence after incubation. b) Illustration of the one-off cell uptake experiment of the DiI@Oil NPs. The fluorescence of the cells remains stable during incubation. Representative CLSM images for incubation of DiI@Polymer NPs (c) and DiI@Oil NPs (d). The same CLSM settings were applied to all groups. Scale bar, 10 μm. The quantitative fluorescence intensity of SKOV3 cells measured by the flow cytometry for the DiI@Polymer (e) and DiI@Oil (f) NPs incubated with cells for 8 h in the one-off cell uptake experiment. g) The quantum yield of DiI@Polymer NPs ($PLGA_{55k}$-PEG_{5k}) with different dye loadings (1, 0.5, 0.1, 0.05, 0.02, and 0.01 wt% DiI). The mean ± s.d. from three independent replicates is shown. N.S. $P > 0.05$, *** $P < 0.001$, analyzed by one-way ANOVA.

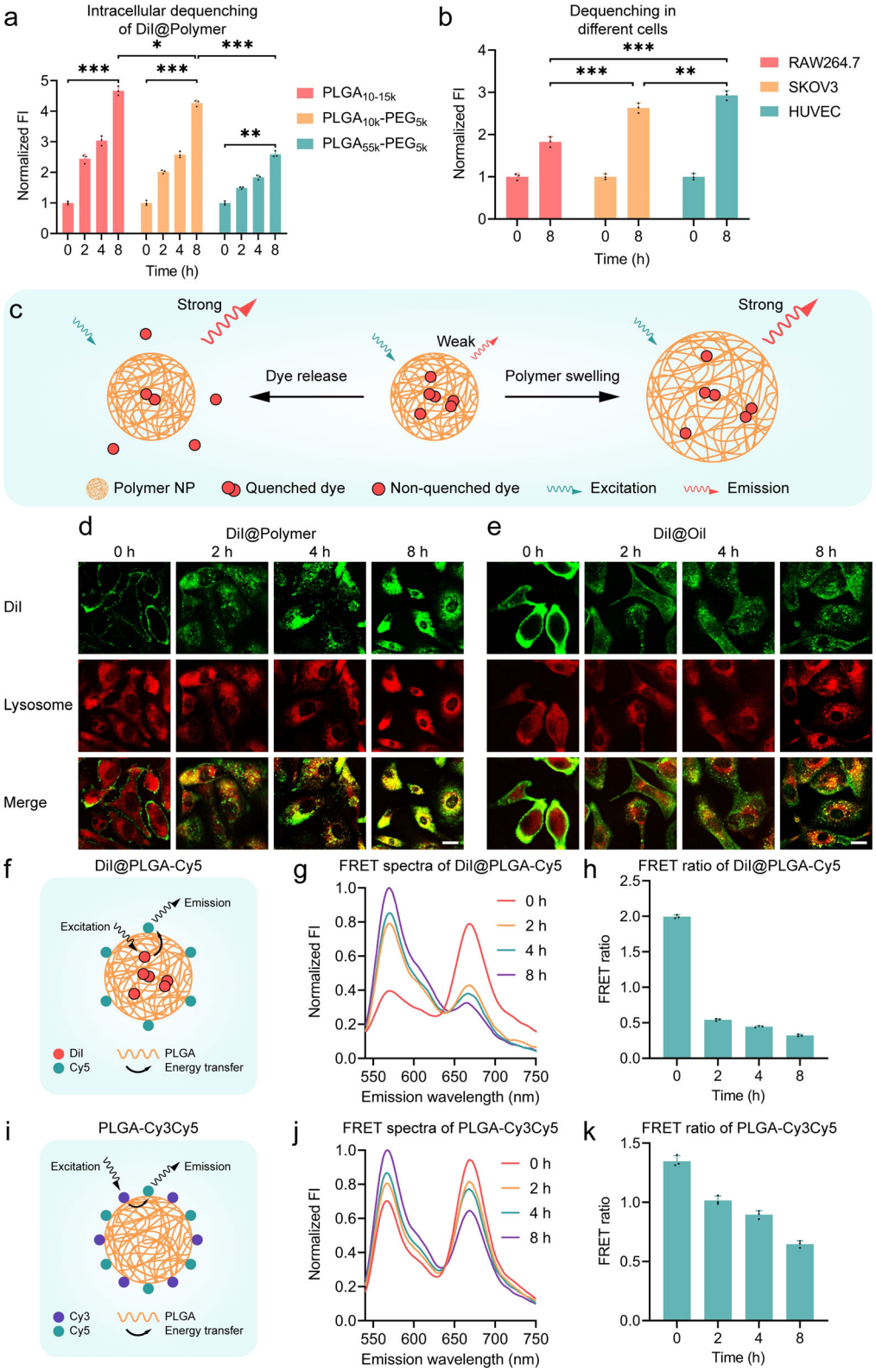

Figure 2. Cell uptake and fluorescence intensity change of DiI@Polymer NPs and DiI@Oil NPs in the one-off cell uptake experiment. a) Intracellular fluorescence change of different DiI@Polymer NPs including $PLGA_{10-15k}$, $PLGA_{10k}$-PEG_{5k}, and $PLGA_{55k}$-PEG_{5k} in cell culture medium. b) Intracellular fluorescence change of $PLGA_{55k}$-PEG_{5k} DiI@Polymer NPs in different cells. c) Schematics of two possible dequenching routes: dye release or polymer swelling. Representative CLSM images showing the internalization of DiI@Polymer NPs (d) and DiI@Oil NPs (e) and their transport to lysosomes, scale bars are 10 μm. The Scheme (f), spectra (g), and FRET ratio (h) of dye release kinetics of the DiI@PLGA-Cy5 NPs (Cy5-labeled DiI-loaded $PLGA_{10-15k}$ NPs) from 0 to 8 h in SKOV3 cells. The Scheme (i), spectra (g), and FRET ratio (k) degradation kinetics of PLGA-Cy3Cy5 NPs (Cy3 and Cy5 co-labeled $PLGA_{10-15k}$ NPs) from 0 to 8 h in SKOV3 cells. The mean ± s.d. from three independent replicates is shown. $*P<0.05$, $**P<0.01$, $***P<0.001$, analyzed by two-way ANOVA.

release of DiI from PLGA-PEG NPs as the presence of PEG could reduce esterase action thus slowing down the degradation of the polymer.[17] These different dequenching kinetics may have interference on the comparison of cell uptake of NPs made from different materials. Furthermore, we incubated the same DiI@Polymer ($PLGA_{55k}$-PEG_{5k}) NPs with three different types of cells, including macrophage (RAW264.7), cancer (SKOV3), and endothelial (HUVECs) cells. We found very different dequenching kinetics (Figure 2b), suggesting the universal phenomenon of the quenching-to-dequenching switch in different cells and different polymer NPs. Based on this phenomenon, we can infer that the fluorescence intensity in biodistribution studies using fluorescence-labeled NPs may not accurately reflect the NP concentration, which may also result from the different digestion kinetics of various cells. We speculate that the quenching-to-dequenching switch could be caused by two possible mechanisms: 1) dye release,[18] so less quenching and recovery of fluorescence signal; and 2) NP swelling thus bigger particle and further distance between dye molecules so less quenching (Figure 2c). Consequently, the different dye release or particle swelling kinetics of different NPs and in different cells would lead to different recovery speeds of the fluorescence intensity.

It is well recognized that intracellular NP degradation primarily occurs at lysosomes,[19] so the process of NP trafficking to lysosomes was monitored using co-localization experiments. Figure 2d,e shows the internalization of DiI@-Polymer NPs and DiI@Oil NPs in the SKOV3 cells and their transport to lysosomes over 8 h. The yellow (merged from red and green) spots in the merge images indicated the co-localization of NPs and lysosomes. The fluorescence intensity increase of DiI@Polymer NPs occurred when the NPs were transferred from the cell membrane into lysosomes, and the DiI started to switch from a quenched state to a non-quenched state at 2 h (Figure 2d; Supporting Information, Figure S8). The DiI@Oil NPs crossed the cell membrane and accumulated at lysosomes (Figure 2e; Supporting Information, Figure S9). However, as the DiI was in the non-quenched state before incubation, the fluorescence intensity did not change along with incubation due to the absence of the state change during incubation.

To further validate our hypothesis about drug release and/or polymer swelling, we designed two FRET experiments to further explore the intracellular behavior of DiI@Polymer NPs in SKOV3 cells. FRET has been widely used for investigating drug release kinetics which involves the energy transfer from one dye to the other, shifting the fluorescence emission. FRET can be used to monitor the integrity and disassembly of fluorescent dye-loaded NPs thus providing valuable spatial and kinetic information.[20] DiI (donor) and Cy5 (acceptor) are a FRET pair, and the FRET effect occurs at the proximity (usually less than 10 nm) between the two dyes (Figure 2f). We synthesized Cy5-labeled DiI loaded $PLGA_{10-15k}$ NPs (DiI@PLGA-Cy5 NPs, Table S1), which were incubated with SKOV3 cells using the one-off cell uptake method. Figure 2g shows that the Cy5 peak was dominating at 0 h, suggesting the successful formation of FRET as a result of the close distance between DiI encapsulated in the NPs and Cy5 on the NP surface. At 2 h, a significant recovery of the DiI emission as well as the dramatic decrease of the FRET ratio suggested the partial separation of DiI and Cy5 (Figure 2h), mainly due to the release of DiI thus the quenching-to-dequenching switch of DiI in DiI@Polymer NPs.

On the other hand, to investigate whether the polymer NPs were swelling and/or degrading during cell uptake experiments, we used Cy3 (donor) and Cy5 (acceptor) as a FRET pair. $PLGA_{10-15k}$-NH_2 polymer was self-assembled to PLGA NP via nanoprecipitation firstly. Then Cy3-NHS and Cy5-NHS (molar ratio 1:1) were conjugated to the PLGA NP, with both Cy3 and Cy5 presenting on the particle surface, so excitation of Cy3 would result in Cy5 emission (Figure 2i and Table S1). Similarly, the PLGA-Cy3Cy5 NPs were incubated with SKOV3 cells. Figure 2j shows that the presence of Cy5 peak at 0 h, suggesting the successful formation of FRET. The steady recovery of the Cy3 emission, as well as the gradual decrease of the FRET ratio from 2 h to 8 h, indicated the gradual separation of Cy3 and Cy5 (Figure 2k) as a result of the NP swelling. Again, it is proved that polymer swelling also plays some roles in the quenching-to-dequenching switch of DiI in DiI@Polymer NPs. These two FRET experiments demonstrate that both DiI release and polymer swelling contributed to the dequenching of DiI in polymer NPs. As different polymers have different swelling and release properties, they exhibit different levels of dequenching in cell experiments.

It is known that long blood circulation time is a prerequisite for targeted drug delivery NPs. So, NP stability in circulation is critical. DiI showed very different fluorescence intensity in PBS and FBS at the same dye concentration (Supporting Information, Figure S10), with FBS showing about 10 times higher fluorescence intensity than that in PBS, demonstrating the effective dye-stabilizing effect of the surface-active biomolecules in FBS such as albumin and lipoproteins,[21] which led to stronger emission of DiI. To mimic the in vivo circulation environment, we further investigated the stability and release kinetics for the 1 wt% DiI@Polymer NPs (DiI-loaded $PLGA_{55k}$-PEG_{5k} NPs) (Figure 3a). 300 $\mu g\,mL^{-1}$ NPs were incubated in FBS at 37 °C with gentle shaking for 48 h. The fluorescence intensity remained almost constant in the first 4 hours, indicating that the particles were stable within a short period of incubation. Then a continuous growth of the fluorescence intensity was observed from 8 to 48 hours, confirming the presence of the quenching-to-dequenching switch of DiI@Polymer NPs in FBS. The dequenching kinetics of the NPs in FBS was slower compared to the intracellular experiments (Figure 2a,b). To investigate the dequenching mechanism of DiI@Polymer NPs in FBS, similar FRET experiments were conducted. The DiI@PLGA-Cy5 and PLGA-Cy3Cy5 NPs were incubated in FBS at 37 °C with gentle shaking for 48 h. Similar trends in FRET spectra and FRET ratio were observed for DiI@PL-GA-Cy5 (Figure 3c,d) and PLGA-Cy3Cy5 NPs (Figure 3e,f), indicating that the increased fluorescence of DiI@Polymer NPs in FBS was attributed mainly to the dequenching of DiI because of dye release and polymer swelling, similar to the cell experiments as discussed above. In contrast, the fluores-

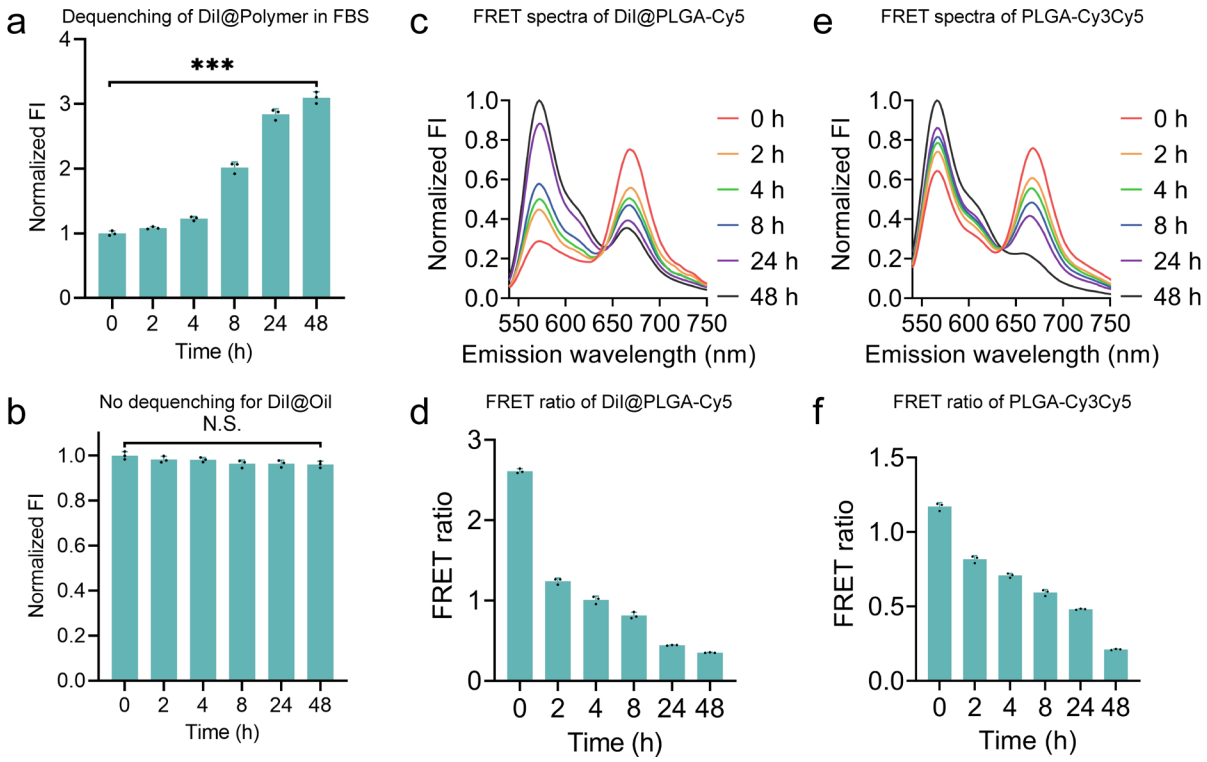

Figure 3. Stability of DiI@Polymer NPs and DiI@Oil NPs in FBS. 1 wt% DiI@Polymer NPs (a) and DiI@Oil NPs (b) were incubated in FBS for 48 h. The fluorescence intensity was measured by a plate reader at different times. The spectra (c) and FRET ratio (d) of DiI@PLGA-Cy5 NPs from 0 h to 48 h in FBS. The spectra (e) and FRET ratio (f) of the PLGA-Cy3Cy5 NPs from 0 h to 48 h in FBS. The mean ± s.d. from three independent replicates is shown. N.S. $P > 0.05$, *** $P < 0.001$, analyzed by one-way ANOVA.

cence intensity of DiI@Oil NPs remained unchanged over time in FBS for 48 h (Figure 3b) due to their good stability in FBS.

The quenching-to-dequenching switch of DiI@Polymer NPs was also observed by other researchers. Trofymchuk et al. reported an increase of the overall average fluorescence intensity of their dye-loaded PLGA NPs in the presence of FBS,[10] as PLGA can be degraded by both acidic pH and enzymes in cells, as well as salt, serum proteins and their catalyzing effect.[22] Temperature also plays a critical role in PLGA degradation, and the elastic modulus of PLGA NPs was found to decrease significantly in water at 37 °C.[23] The swelling and/or degradation mechanism of PLGA NPs in FBS could also be explained by the adsorption of serum proteins onto the NP surface thus reducing the stability of particles.[24] The catalyzing effect of divalent ions (Ca^{2+}, Mg^{2+}) in FBS might also accelerate the degradation of PLGA.[25]

To examine whether this quenching-to-dequenching switch also occurs in vivo, we synthesized 1 wt% DiR@Polymer NPs (1,1′-dioctadecyl-3,3,3′,3′-tetramethylindotricarbocyanine iodide-loaded $PLGA_{55k}$-PEG_{5k} NPs) and injected them into mice (Supporting Information, Table S1). The whole-body fluorescence intensity of mice was recorded over time (Figure 4a,b). From 0 to 6 h, a gradual reduction of the fluorescence intensity was observed due to the rapid clearance of the NPs in vivo. However, the fluorescence intensity of the whole body underwent a significant increase from 6 to 24 h, indicating that the fluorescence increase owing to the dequenching surpassed the fluorescence decrease resulting from the clearance of the dyes, thus an overall increase of the fluorescence intensity. After 24 h, the clearance of the DiR dominated again and led to a steady decrease. This decrease-increase-decrease trend was clearly observed from images of a representative mouse and the average fluorescence intensity of the whole body for all 4 mice.

Additionally, we synthesized DiR@Oil NPs (DiR-loaded oil-core silica-shell NPs) and injected them into mice (Supporting Information, Table S1). From 0 to 72 h, a gradual reduction of the fluorescence intensity was observed and no significant increase of whole-body fluorescence intensity of mice was observed at any time points, suggesting the absence of the state switch of DiR of the DiR@Oil NPs (Figure 4c,d) as DiR was dissolved in the oil core of the DiR@Oil NPs thus no quenching effect (Supporting Information, Figure S11). The in vivo environment is complex consisting of both serum circulation and cell uptake. Therefore, similar to our in vitro results for cell experiment (Figure 2) and FBS experiment (Figure 3), the dequenching of DiR@Polymer NPs in vivo was primarily due to dye release and the swelling and/or degradation of polymers.

The presence of this quenching-to-dequenching switch in serum, cells as well as in vivo raise a significant question about the reliability and accuracy of using dye-labeling methods to investigate cell uptake and biodistribution studies. Different release and swelling kinetics of different NP further complicate the problem. Therefore, it is critical to develop more accurate methods to address these challenges. Herein, we present two possible solutions.

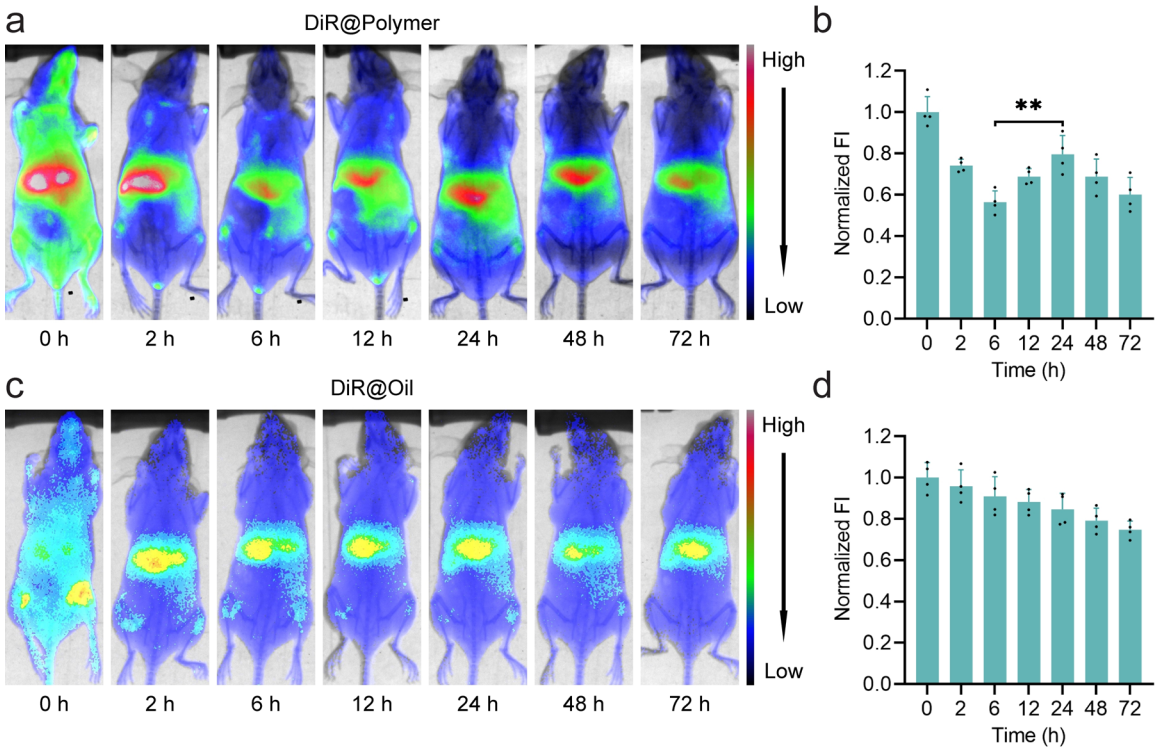

Figure 4. Comparison of DiR@Polymer NPs and DiR@Oil NPs in vivo. DiR@Polymer NPs and DiR@Oil NPs were injected into mice, and fluorescence photographs were taken at different times. a) Photographs of one representative mouse in (b), the DiR@Polymer NPs showing obvious fluorescence intensity increase from 6 h to 24 h in vivo. c) Photographs of one representative mouse in (d) and the DiR@Oil NPs showing no fluorescence intensity increase in vivo. The same equipment settings were applied for all photographs and the fluorescence intensity of the whole body was analyzed by ImageJ. Data are reported as mean ± s.d. ($n = 4$). $^{**}P < 0.01$, analyzed by one-way ANOVA.

Firstly, lowering dye loading in NPs might offer a possible solution to minimize the dequenching (Figure 5a). The DiI@Polymer NPs with dye loading from 1 to 0.02 wt % were incubated with SKOV3 cells (Supporting Information, Table S1). The dequenching was observed from 1 wt % down to 0.1 wt % DiI loadings, and the dequenching degree correlates reversely with the dye loading. We did not observe any quenching at 0.05 % and 0.02 % DiI loading, whereas the fluorescence signal was very low due to the low dye concentration. Therefore, lowering dye loading is able to reduce dye quenching, but also decrease fluorescence intensity significantly as well, which compromises the sensitivity and accuracy of experiments, so not ideal for in vitro and in vivo studies.

The second method is called the medium analysis method. Basically, instead of analyzing the fluorescence intensity of cells as done in traditional methods, the medium containing NPs is collected and then dissolved in solvents to quantify the NP amount in the medium, then calculate back to get the NP uptake result. In contrast to the traditional method using flow cytometry (Figure 5b), we prepared two NP samples with one as the control group containing no cells and the other one as the test group (Figure 5c). The NPs in the test group were incubated with cells as usual, whereas the NPs in the control group were incubated just with the medium. After incubation, both media containing NPs were analyzed. The difference between fluorescence intensities from these two groups was determined as the cell uptake of NPs. This method eliminates the impacts from the dequenching as well as the quenching effect of the loaded dyes, so it provides a more accurate quantification method that does not require very careful consideration of the dye loading or dye concentration. By replacing the dye with drugs, this method allows the direct quantification of cell uptake of drug-loaded NPs.

As a demonstration, we used three different DiI@Polymer NPs, DiI@PLGA$_{10–15k}$, DiI@PLGA$_{10k}$-PEG$_{5k}$, and DiI@PLGA$_{55k}$-PEG$_{5k}$ NPs, all with 1 wt % DiI loading. They were incubated with SKOV3 cells at the same DiI concentration, and then their cell uptakes were quantified using both the traditional flow cytometry method and the medium analysis method (Figure 5d). After normalization against the DiI@PLGA$_{10k}$-PEG$_{5k}$ group, we can see very different results from these two methods. For both the DiI@PLGA$_{10–15k}$ and DiI@PLGA$_{55k}$-PEG$_{5k}$ groups, the flow cytometry method gave higher uptake than the medium analysis method. If we compared the NP uptake results using these two different methods, we would draw very different conclusions. But as we discussed, the medium analysis method gives more accurate results showing that the DiI@PLGA$_{10–15k}$ can be taken up by SKOV3 cells more preferably followed by DiI@PLGA$_{10k}$-PEG$_{5k}$ then DiI@PLGA$_{55k}$-PEG$_{5k}$ NPs.

Similarly, for biodistribution studies of dye-labeled NPs in vivo by fluorescent imaging, similar medium analysis methods could be applied, which has already been used in classical in vivo drug distribution studies. Typically, the drug is extracted from homogenized tissues using a solvent and then analyzed

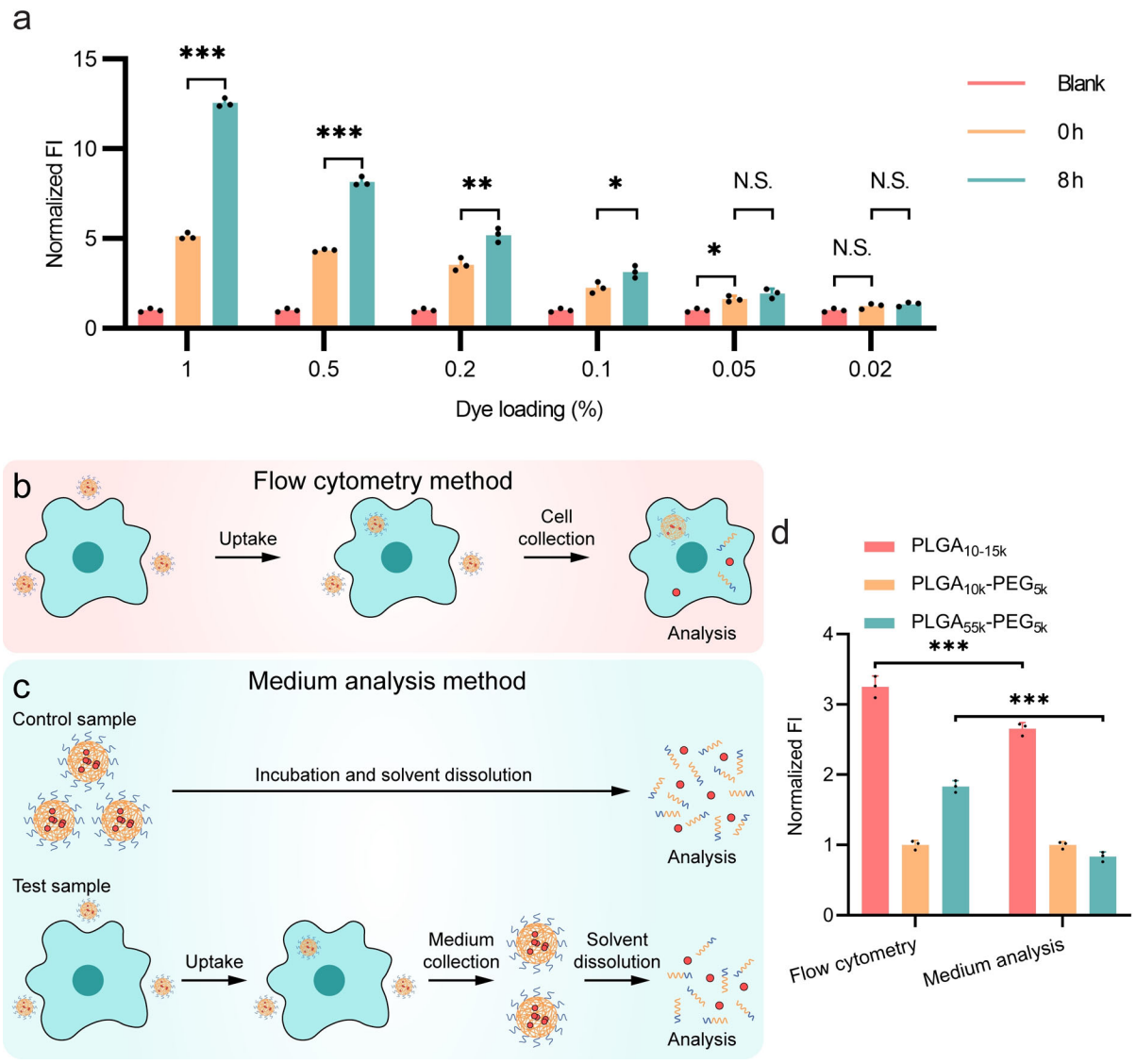

Figure 5. Two proposed strategies to minimize dye quenching effect. 1) Lower dye loading; 2) medium analysis. The dequenching level (a) in different dye loadings with the same NP concentration for the NP suspensions. $PLGA_{55k}$-PEG_{5k} NP suspensions with 1, 0.5, 0.1, 0.05, and 0.02 wt% DiI loadings were incubated with SKOV3 cells using the one-off cell uptake method. b) The traditional flow cytometry (FC) method analyzes the fluorescence from cells to determine the cell uptake of NPs containing dye, which may lead to false results due to the dequenching. c) A more accurate medium analysis (MA) method to determine cell uptake of NPs loading hydrophobic dyes. The control and test samples are prepared. After incubation, the medium containing free NPs is collected, and solvents are then added to dissolve the dye to eliminate the ACQ effect. Subsequently, the fluorescence intensity difference of the control and test sample is measured as the cell uptake of NPs. d) Cell uptake of DiI@Polymer NPs fabricated using different polymers: $PLGA_{10-15k}$, $PLGA_{10k}$-PEG_{5k}, and $PLGA_{55k}$-PEG_{5k}, determined by the FC and MA methods. The cell uptake was normalized to the $PLGA_{10k}$-PEG_{5k} group. These two different methods demonstrated different uptake results. The mean ± s.d. from three independent replicates is shown for (a) and (d). N.S.$P > 0.05$, *$P < 0.05$, **$P < 0.01$, ***$P < 0.001$, analyzed by one-way (a) and two-way (d) ANOVA.

to determine its concentration. This is more reliable, and its concept is the same as the medium analysis method we propose here. Compared to the first method that reduces dye loading, the second method offers a more accurate and reliable method for quantification of cell uptake and biodistribution studies, as well as comparative studies of different NP systems both in vitro and in vivo.

Conclusion

We have demonstrated a ubiquitous quenching-to-dequenching switch of dye-labeled NPs especially for dye-labeled polymer NPs, which occurs in both in vitro quantitative cell uptake and in vivo biodistribution studies. When these dye-labeled NPs interact with biological systems (cell culture medium, cells, and organs to animals), dye undergoes a quenching-to-dequenching switch, leading to a significant increase of fluorescence intensity. This switch is mainly due to

dye release and polymer swelling and/or degradation. Many factors affect the kinetics of the dequenching including NP materials, local environments, and cell types. These phenomena make it problematic to directly compare NP cell uptake and biodistribution using traditional quantification methods, as the fluorescence intensity becomes dynamic owing to dequenching thus cannot accurately represent NP concentration. To address the quenching and dequenching problems, we proposed two possible solutions: using lower dye loading and using medium analysis for quantifying cell uptake of NPs. This study highlights that it is vital to design in vitro cell uptake and in vivo biodistribution experiments carefully, especially for comparing different NP systems. On the other hand, although the quenching-to-dequenching switch is undesirable for comparative studies, it provides new opportunities for investigating the degradation of NPs and the release of dyes from NPs.

Acknowledgements

This work was supported by the Australian Research Council (FT140100726 and DP200101238). The authors acknowledge Lei Yu, Dr. Rui Ran, Dr. Haofei Wang, Dr. David Wibowo, Dr. Arjun Seth, and Barb Arnts for their help and advice on experiments. The authors acknowledge the facilities, and the scientific and technical assistance, of the Australian Microscopy & Microanalysis Research Facility at the Centre for Microscopy and Microanalysis, The University of Queensland. This work was performed in part at the Queensland node of the Australian National Fabrication Facility, a company established under the National Collaborative Research Infrastructure Strategy to provide nano and microfabrication facilities for Australia's researchers.

Conflict of interest

The authors declare no conflict of interest.

Keywords: biodistribution · cell uptake · fluorescence · nanoparticles · quenching

[1] a) M. J. Mitchell, M. M. Billingsley, R. M. Haley, M. E. Wechsler, N. A. Peppas, R. Langer, *Nat. Rev. Drug Discovery* **2020**, *19*, 1 – 24; b) D. Nie, Z. Dai, J. Li, Y. Yang, Z. Xi, J. Wang, W. Zhang, K. Qian, S. Guo, C. Zhu, *Nano Lett.* **2020**, *20*, 936 – 946; c) F. Y. Han, Y. Liu, V. Kumar, W. Xu, G. Yang, C.-X. Zhao, T. M. Woodruff, A. K. Whittaker, M. T. Smith, *Int. J. Pharm.* **2020**, *581*, 119291.

[2] a) F. Tang, L. Li, D. Chen, *Adv. Mater.* **2012**, *24*, 1504 – 1534; b) H. Kettiger, A. Schipanski, P. Wick, J. Huwyler, *Int. J. Nanomed.* **2013**, *8*, 3255; c) E. Blanco, H. Shen, M. Ferrari, *Nat. Biotechnol.* **2015**, *33*, 941.

[3] a) J. Wang, X. Tao, Y. Zhang, D. Wei, Y. Ren, *Biomaterials* **2010**, *31*, 4426 – 4433; b) T. Dos Santos, J. Varela, I. Lynch, A. Salvati, K. A. Dawson, *Small* **2011**, *7*, 3341 – 3349; c) V. P. Torchilin, *Nat. Rev. Drug Discovery* **2014**, *13*, 813; d) H.-F. Wang, R. Ran, Y. Liu, Y. Hui, B. Zeng, D. Chen, D. A. Weitz, C.-X. Zhao, *ACS Nano* **2018**, *12*, 11600 – 11609; e) H. Cao, Y. Yang, J. Li, *Aggregate* **2020**, *1*, 69 – 79; f) M. Kang, Z. Zhang, N. Song, M. Li, P. Sun, X. Chen, D. Wang, B. Z. Tang, *Aggregate* **2020**, *1*, 80 – 106.

[4] T. Etrych, H. Lucas, O. Janoušková, P. Chytil, T. Mueller, K. Mäder, *J. Controlled Release* **2016**, *226*, 168 – 181.

[5] a) C. He, Y. Hu, L. Yin, C. Tang, C. Yin, *Biomaterials* **2010**, *31*, 3657 – 3666; b) A. Salvati, A. S. Pitek, M. P. Monopoli, K. Prapainop, F. B. Bombelli, D. R. Hristov, P. M. Kelly, C. Åberg, E. Mahon, K. A. Dawson, *Nat. Nanotechnol.* **2013**, *8*, 137; c) G. Yang, Y. Liu, H. Wang, R. Wilson, Y. Hui, L. Yu, D. Wibowo, C. Zhang, A. K. Whittaker, A. P. Middelberg, *Angew. Chem. Int. Ed.* **2019**, *58*, 14357 – 14364; *Angew. Chem.* **2019**, *131*, 14495 – 14502.

[6] a) Y. Liu, G. Yang, T. Baby, D. Chen, D. A. Weitz, C. X. Zhao, *Angew. Chem. Int. Ed.* **2020**, *59*, 4720 – 4728; *Angew. Chem.* **2020**, *132*, 4750 – 4758; b) A. M. Syed, P. MacMillan, J. Ngai, S. Wilhelm, S. Sindhwani, B. R. Kingston, J. L. Wu, P. Llano-Suárez, Z. P. Lin, B. Ouyang, *Nano Lett.* **2020**, *20*, 1362 – 1369.

[7] a) Y. Singh, J. G. Meher, K. Raval, F. A. Khan, M. Chaurasia, N. K. Jain, M. K. Chourasia, *J. Controlled Release* **2017**, *252*, 28 – 49; b) Y. Hui, X. Yi, D. Wibowo, G. Yang, A. P. Middelberg, H. Gao, C.-X. Zhao, *Sci. Adv.* **2020**, *6*, eaaz4316.

[8] J. Qi, X. Hu, X. Dong, Y. Lu, H. Lu, W. Zhao, W. Wu, *Adv. Drug Delivery Rev.* **2019**, *143*, 206 – 225.

[9] F. Meng, J. Wang, Q. Ping, Y. Yeo, *ACS Nano* **2018**, *12*, 6458 – 6468.

[10] K. Trofymchuk, J. Valanciunaite, B. Andreiuk, A. Reisch, M. Collot, A. S. Klymchenko, *J. Mater. Chem. B* **2019**, *7*, 5199 – 5210.

[11] a) M. N. Holme, I. A. Fedotenko, D. Abegg, J. Althaus, L. Babel, F. Favarger, R. Reiter, R. Tanasescu, P.-L. Zaffalon, A. Ziegler, *Nat. Nanotechnol.* **2012**, *7*, 536; b) I.-h. Oh, H. S. Min, L. Li, T. H. Tran, Y.-k. Lee, I. C. Kwon, K. Choi, K. Kim, K. M. Huh, *Biomaterials* **2013**, *34*, 6454 – 6463.

[12] Y. Liu, G. Yang, S. Jin, R. Zhang, P. Chen, Tengjisi, L. Wang, D. Chen, D. A. Weitz, C.-X. Zhao, *Angew. Chem. Int. Ed.* **2020**, *59*, 20065 – 20074; *Angew. Chem.* **2020**, *132*, 20240 – 20249.

[13] a) J. Huang, H. Zhang, Y. Yu, Y. Chen, D. Wang, G. Zhang, G. Zhou, J. Liu, Z. Sun, D. Sun, *Biomaterials* **2014**, *35*, 550 – 566; b) A. M. Milosevic, L. Rodriguez-Lorenzo, S. Balog, C. A. Monnier, A. Petri-Fink, B. Rothen-Rutishauser, *Angew. Chem. Int. Ed.* **2017**, *56*, 13382 – 13386; *Angew. Chem.* **2017**, *129*, 13567 – 13571; c) J. Xue, Z. Zhao, L. Zhang, L. Xue, S. Shen, Y. Wen, Z. Wei, L. Wang, L. Kong, H. Sun, *Nat. Nanotechnol.* **2017**, *12*, 692; d) J. Xu, Y. Liu, Y. Li, H. Wang, S. Stewart, K. Van der Jeught, P. Agarwal, Y. Zhang, S. Liu, G. Zhao, *Nat. Nanotechnol.* **2019**, *14*, 388.

[14] a) J. B. Birks, *Aromatic Molecules*, *Vol. 704*, Wiley, New York, **1970**; b) W. Z. Yuan, P. Lu, S. Chen, J. W. Lam, Z. Wang, Y. Liu, H. S. Kwok, Y. Ma, B. Z. Tang, *Adv. Mater.* **2010**, *22*, 2159 – 2163.

[15] a) H. Chen, S. Kim, L. Li, S. Wang, K. Park, J.-X. Cheng, *Proc. Natl. Acad. Sci. USA* **2008**, *105*, 6596 – 6601; b) J. M. Rosenholm, E. Peuhu, J. E. Eriksson, C. Sahlgren, M. Lindén, *Nano Lett.* **2009**, *9*, 3308 – 3311; c) A. Roy, M. J. Ernsting, E. Undzys, S.-D. Li, *Biomaterials* **2015**, *52*, 335 – 346; d) Y. Liu, Y. Hui, R. Ran, G. Z. Yang, D. Wibowo, H. F. Wang, A. P. Middelberg, C. X. Zhao, *Adv. Healthcare Mater.* **2018**, *7*, 1800106; e) J. Feng, S. Lepetre-Mouelhi, A. Gautier, S. Mura, C. Cailleau, F. Coudore, M. Hamon, P. Couvreur, *Sci. Adv.* **2019**, *5*, eaau5148.

[16] Y. Hui, D. Wibowo, Y. Liu, R. Ran, H.-F. Wang, A. Seth, A. P. Middelberg, C.-X. Zhao, *ACS Nano* **2018**, *12*, 2846 – 2857.

[17] G. Fontana, M. Licciardi, S. Mansueto, D. Schillaci, G. Giammona, *Biomaterials* **2001**, *22*, 2857 – 2865.

[18] D. W. Löwik, J. C. van Hest, *Chem. Soc. Rev.* **2004**, *33*, 234 – 245.

[19] A. Lesniak, A. Salvati, M. J. Santos-Martinez, M. W. Radomski, K. A. Dawson, C. Åberg, *J. Am. Chem. Soc.* **2013**, *135*, 1438 – 1444.

[20] a) R. M. Clegg, *Lab. Tech. Biochem. Mol. Biol.* **2009**, *33*, 1 – 57; b) D. M. Charron, G. Zheng, *Nano Today* **2018**, *18*, 124 – 136.
[21] F. Contu, B. Elsener, H. Böhni, *J. Biomed. Mater. Res.* **2002**, *62*, 412 – 421.
[22] a) Q. Cai, G. Shi, J. Bei, S. Wang, *Biomaterials* **2003**, *24*, 629 – 638; b) Y. Zhang, S. Zale, L. Sawyer, H. Bernstein, *J. Biomed. Mater. Res.* **1997**, *34*, 531 – 538.
[23] N. Alsharif, B. Eshaghi, B. M. Reinhard, K. A. Brown, *Nano Lett.* **2020**, *20*, 7536 – 7542.
[24] Y. Xu, C. S. Kim, D. M. Saylor, D. Koo, *J. Biomed. Mater. Res. Part B* **2017**, *105*, 1692 – 1716.
[25] S. Fredenberg, M. Reslow, A. Axelsson, *Pharm. Dev. Technol.* **2007**, *12*, 563 – 572.

Manuscript received: February 3, 2021
Revised manuscript received: March 15, 2021
Accepted manuscript online: April 1, 2021
Version of record online: ■■ ■■, ■■■■

Research Articles

Fluorescence Quenching

G. Yang, Y. Liu, Y. Hui, D. Chen, D. A. Weitz, C.-X. Zhao* ____ ▮▮▮▮–▮▮▮▮

Implications of Quenching-to-Dequenching Switch in Quantitative Cell Uptake and Biodistribution of Dye-Labeled Nanoparticles

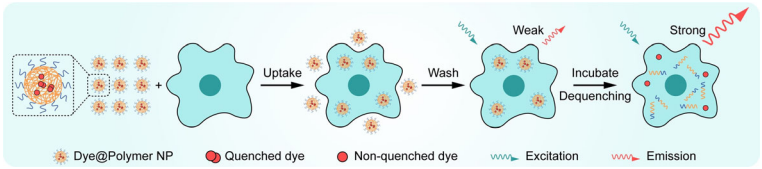

A ubiquitous quenching-to-dequenching switch of dye-labeled nanoparticles in vitro and in vivo is presented. When dye-labeled nanoparticles interact with biological systems (cell culture medium, cells, and organs to animals), the dye undergoes the switch, causing a significant increase of fluorescence intensity.